01 Jul 2009

Temporal Geophysical Signatures from Contaminant-Mass Remediation

Vukenkeng Che-Alota

Estella A. Atekwana
Missouri University of Science and Technology, atekwana@mst.edu

Eliot A. Atekwana
Missouri University of Science and Technology

William August Sauck

et. al. For a complete list of authors, see https://scholarsmine.mst.edu/geosci_geo_peteng_facwork/1291

Recommended Citation

V. Che-Alota et al., "Temporal Geophysical Signatures from Contaminant-Mass Remediation," *Geophysics*, vol. 74, no. 4, pp. B113-B123, Society of Exploration Geophysicists, Jul 2009.
The definitive version is available at https://doi.org/10.1190/1.3139769

GEOPHYSICS, VOL. 74, NO. 4 (JULY-AUGUST 2009); P. B113–B123, 8 FIGS.
10.1190/1.3139769

Case History

Temporal geophysical signatures from contaminant-mass remediation

Vukenkeng Che-Alota[1], Estella A. Atekwana[1], Eliot A. Atekwana[1], William A. Sauck[2], and D. Dale Werkema Jr.[3]

ABSTRACT

We have previously documented changes in bulk electrical conductivity, self-potential (SP), and ground-penetrating-radar (GPR) reflections in a field setting caused by biogeochemical transformations of hydrocarbon-contaminated media. These transformations are associated with hydrocarbon biodegradation. The results of surface geophysical surveys acquired in 1996, 2003, and 2007 document changes in geophysical signatures associated with removing hydrocarbon mass in the contaminated zone. Initial investigations in 1996 showed that relative to background, the contaminated area was characterized by higher bulk electrical conductivity, positive SP anomaly, and attenuated GPR reflections. Repeated surveys in 2003 and 2007 over the contaminated area showed that in 2007, the bulk electrical conductivity had reverted to near-background conditions, the positive SP anomaly became more negative, and the zone of attenuated GPR reflections showed increased signal strength. Removal of hydrocarbon mass in the vadose zone over the plume by a soil vapor-extraction system installed in 2001 was primarily responsible for the changing geophysical responses. Although chemical data from groundwater showed a 3-m-thick conductive plume in 2007, the plume was not imaged by electrical resistivity. Forward modeling suggests that apparent bulk electrical conductivity of the saturated zone plume has to be three to five times higher than background values to be imaged by electrical resistivity. We suggest that removing hydrocarbon-contaminant-mass reduction by natural or engineered bioremediation can be imaged effectively by temporal geophysical surveys.

INTRODUCTION

Hydrocarbon contamination of groundwater from spills and leaky underground storage tanks threatens groundwater resources. Over the last decade, the use of noninvasive geophysical techniques has been instrumental in detecting and delineating subsurface zones of hydrocarbon contamination. We have documented anomalous increases in bulk electrical conductivity over areas of hydrocarbon contamination (e.g., Sauck et al., 1998; Atekwana et al., 2000; Werkema et al., 2003; Atekwana et al., 2004a; Atekwana et al., 2004b, Atekwana et al., 2004d; Atekwana et al., 2005). Other geophysical studies have also characterized subsurface hydrocarbon contamination effectively using electrical resistivity techniques (e.g., Benson et al., 1997; Halihan et al., 2005; Kaufmann and Deceuster, 2007; Yang et al., 2007), ground-penetrating radar (GPR) (e.g., Daniels et al., 1995; Bermejo et al., 1997; Bradford, 2007; Cassidy, 2007, 2008) and self-potential (SP) (e.g., Minsley et al., 2007).

The characteristic geophysical response of hydrocarbon-contaminated media has been attributed to a variety of physical, chemical, and biological mechanisms. For example, Sauck (2000) attributes the increase in the bulk electrical conductivity to higher pore-water conductivity resulting from aquifer solids weathered by the organic and carbonic acids produced during biodegradation. Other geophysical studies suggest a variety of mechanisms primarily related to microbial alteration of the hydrocarbon and the host media (e.g., Atekwana et al., 2004c; Atekwana et al., 2004d; Minsley et al., 2007). Re-

Manuscript received by the Editor 15 September 2008; revised manuscript received 7 January 2009; published online 26 June 2009.
[1]Oklahoma State University, Boone Pickens School of Geology, Stillwater, Oklahoma, U.S.A. E-mail: vukenkeng.che_alota@okstate.edu; estella.atekwana@okstate.edu; eliot.atekwana@okstate.edu.
[2]Western Michigan University, Department of Geosciences, Kalamazoo, Michigan, U.S.A. E-mail: bill.sauck@wmich.edu.
[3]U. S. Environmental Protection Agency, Office of Research and Development, Las Vegas, Nevada, U.S.A. E-mail: werkema.d@epamail.epa.gov.

cent geophysical studies also suggest that the growth of microorganisms, their attachment to mineral surfaces, and the formation of biofilms are important in the type of geophysical response observed (e.g., Abdel Aal et al., 2004, 2006; Davis et al., 2006; Abdel Aal et al., 2009). Regardless of the mechanism that causes the geophysical response, fundamental changes in physical properties clearly were responsible for the success of geophysical investigations.

We illustrate our problem with a schematic (Figure 1) of the processes we investigated. Although we use bulk electrical conductivity as a measure of the geophysical response, a similar approach can be constructed for any geophysical technique that has been applied successfully to hydrocarbon contamination (e.g., electrical resistivity, GPR, SP). At the initial stage of contamination, fresh spills are associated with a decrease in the bulk electrical conductivity (e.g., Endres and Redman, 1996; Yang et al., 2007) because of the resistive nature of the petroleum hydrocarbon (stage A). As microbial degradation of the contaminant mass is initiated, microbial colonization of mineral surfaces and the production of organic and carbonic acid enhance mineral weathering within the contaminated aquifer (e.g., Cozzarelli et al., 1990; Baedecker et al., 1993; McMahon et al., 1995; Bennett et al., 1996). This increases the electrical conductivity of the pore fluids (electrolytic conductivity) and increases the bulk electrical conductivity (e.g., Sauck, 2000; Atekwana et al., 2004a; Atekwana et al., 2004c; Atekwana et al., 2004d). In addition, the microbial cells attach to mineral surfaces and biofilm grow and proliferate (e.g., Abdel Aal et al., 2004, 2006; Davis et al., 2006) adding to the bulk electrical conductivity by increasing the interfacial conductivity component (stage B).

Over time, the bulk electrical conductivity of the contaminated zone increases to some peak value and reaches a steady state related to the availability of terminal electron acceptors, the organic-carbon-source concentration, and microbial activity (stage C). With continuous removal of the contaminant mass by natural attenuation or engineered bioremediation, we predict a decrease in microbial activity and accompanying changes induced directly or indirectly by microbial activities in the contaminated environment. We suggest there will be a decrease in bulk electrical conductivity to lower values close to or at prespill conditions (stage D). The temporal frame

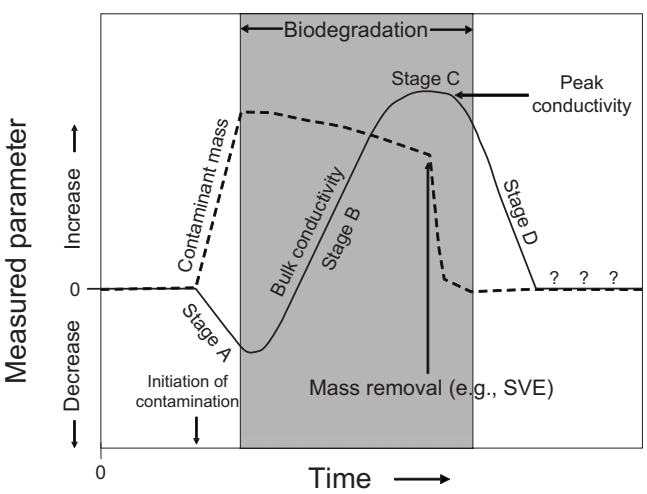

Figure 1. Conceptual model of petroleum hydrocarbon contamination, illustrating the temporal behavior of bulk electrical conductivity from contaminant mass reduction by biodegradation, natural attenuation, or engineered remediation.

required for these changes to occur depends on several factors, such as the mass of hydrocarbon contamination, relative ease of contaminant breakdown, presence of indigenous microorganisms, availability of terminal electron acceptors, mineralogy of the aquifer, and the hydrogeology of the site.

It is important to consider whether geophysical signatures associated with hydrocarbon biodegradation will revert to background conditions with removal of the contaminant mass (stage D, see Figure 1) and if geophysical techniques can be used to ascertain such changes. Published results of field geophysical investigations of hydrocarbon contamination show a variety of geophysical responses (e.g., Daniels et al., 1995; Bermejo et al., 1997; Benson et al., 1997, de la Vega et al., 2003; Cassidy et al., 2007; Kaufmann and Deceuster, 2007; Yang et al., 2007). Thus, it is not apparent from published geophysical surveys whether the measured response indicates a specific state of hydrocarbon-contamination evolution, i.e., stages B, C, or D. Understanding the geophysical response arising from hydrocarbon-contaminant-mass attenuation is likely to make noninvasive geophysical surveys a regular regimen in approaches that monitor natural and engineered bioremediation.

Our objective was to measure changes in geophysical signatures arising from the effects of hydrocarbon-source removal in the vadose zone at a site undergoing biodegradation. A soil vapor-extraction system (SVE) installed within the source zone provided an opportunity to investigate geophysical signatures associated with contaminant-mass reduction. We used three methods: bulk electrical resistivity, SP, and GPR. We chose these methods because they had been used at the study site and are sensitive to microbial-induced changes in physical properties at hydrocarbon-contaminated sites.

SITE GEOLOGY AND SITE HISTORY

This study was conducted at Fire Training Area 2 (FT-02) located on the decommissioned Wurtsmith Air Force Base in Oscoda, Michigan, U.S.A. (Figure 2). Wurtsmith Air Force Base lies on an 8-km-wide sandy plain, which is part of the Oscoda Lake Plain (U. S. Geological Survey, 1991).

The subsurface stratigraphy consists of well-sorted, fine-to-medium sands that grade downward to gravel. Underlying the sand and gravel deposits at approximately 20 m is a brown-to-gray lacustrine silty clay unit ranging in thickness from about 6.1–30.5 m. The silty clay unit is underlain by a thin glacial till deposit that rests on bedrock consisting of Mississippian Marshal Sandstone and Coldwater Shale. Average depth to water table at the site ranges from 3.7 to 5.3 m, and groundwater flow is to the southeast, toward a large wetland located 366 m in the floodplain of the Au Sable River. Aquifer hydraulic conductivity is 3.47×10^{-4} m/s to 5.32 $\times 10^{-4}$ m/s, and groundwater flow varies from 0.03 to 0.2 m/day (U. S. Geological Survey, 1991).

The U. S. Air Force used the FT-02 site for biweekly fire training for 33 years, from 1958 to 1991. Typical activities included combustion of several thousand liters of jet fuel and other hydrocarbon fuels. Waste and other combustion products seeped directly into the ground. In 1982, a concrete fire-containment basin with an oil-water separator was installed to reduce the amount of fuel seeping into the ground. However, an unknown quantity of fuel had already infiltrated the subsurface. In the early '90s, the site was used as the National Center for Integrated Bioremediation Research and Development (NCIBRD) and has been the focus of several geophysical and geochemical investigations (e.g., Chapelle et al., 1996; Bermejo et

al., 1997; Sauck et al., 1998; Skubal et al., 1999; McGuire et al., 2000; Skubal et al., 2001; Moody et al., 2003; Bradford, 2007). A contaminant light nonaqueous-phase liquid (LNAPL) plume (Figure 2) has been defined by chemical analyses of groundwater, spreading up- and downgradient relative to the concrete pad. In the downgradient direction, most contamination is concentrated in the upper portion of the water table and within the capillary fringe (e.g., Sauck et al., 1998; McGuire et al., 2000; Skubal et al., 2001), with significant impact of the vadose zone occurring near the source area. The size of the FT-02 plume defined geochemically is approximately 75–100 m wide and extends 30 m upgradient and about 450 m downgradient to the southeast of the source area (Figure 2).

METHODS

Geophysical surveys

Geophysical surveys were conducted near the source area. We conducted electrical-resistivity surveys and GPR along the same profile and the SP survey in a grid (Figure 2). Our survey lines and grids, based on permanent grid markers established by the University of Michigan, are located at 15.24-m intervals across the entire site. Electrical-resistivity surveys (see Figure 2 for profile location) conducted in 1996 and 2003 used a dipole-dipole array with a 10-m electrode spacing. A single-channel IRIS Syscal R2 resistivity system with four electrodes was used to acquire the data. In 2007, a dipole-dipole resistivity array was conducted at 3-m electrode spacing using a 10-channel IRIS Syscal proresistivity system with 72 electrodes. Apparent-resistivity data were inverted using RES2DINV (Geotomo software), and a least-squares inversion technique was used for the inversion subroutine (Loke and Baker, 1996).

Although the resistivity data for 2007 were collected at 3-m electrode spacing, the main difference compared to 1996 and 2003 data collected at 10-m spacing was formation resolution and depth imaged. Data acquired at 3-m spacing had a higher resolution. Resampling the data at an equivalent 10-m spacing and modeling the data showed no major difference in the resistivity structure of the subsurface. In terms of depth imaging, a survey using a 10-m spacing is about 50 m, although the 3-m-electrode-spacing survey images about 15 m of the subsurface. Because of differences in acquisition parameters (10-m versus 3-m electrode spacing), a difference image

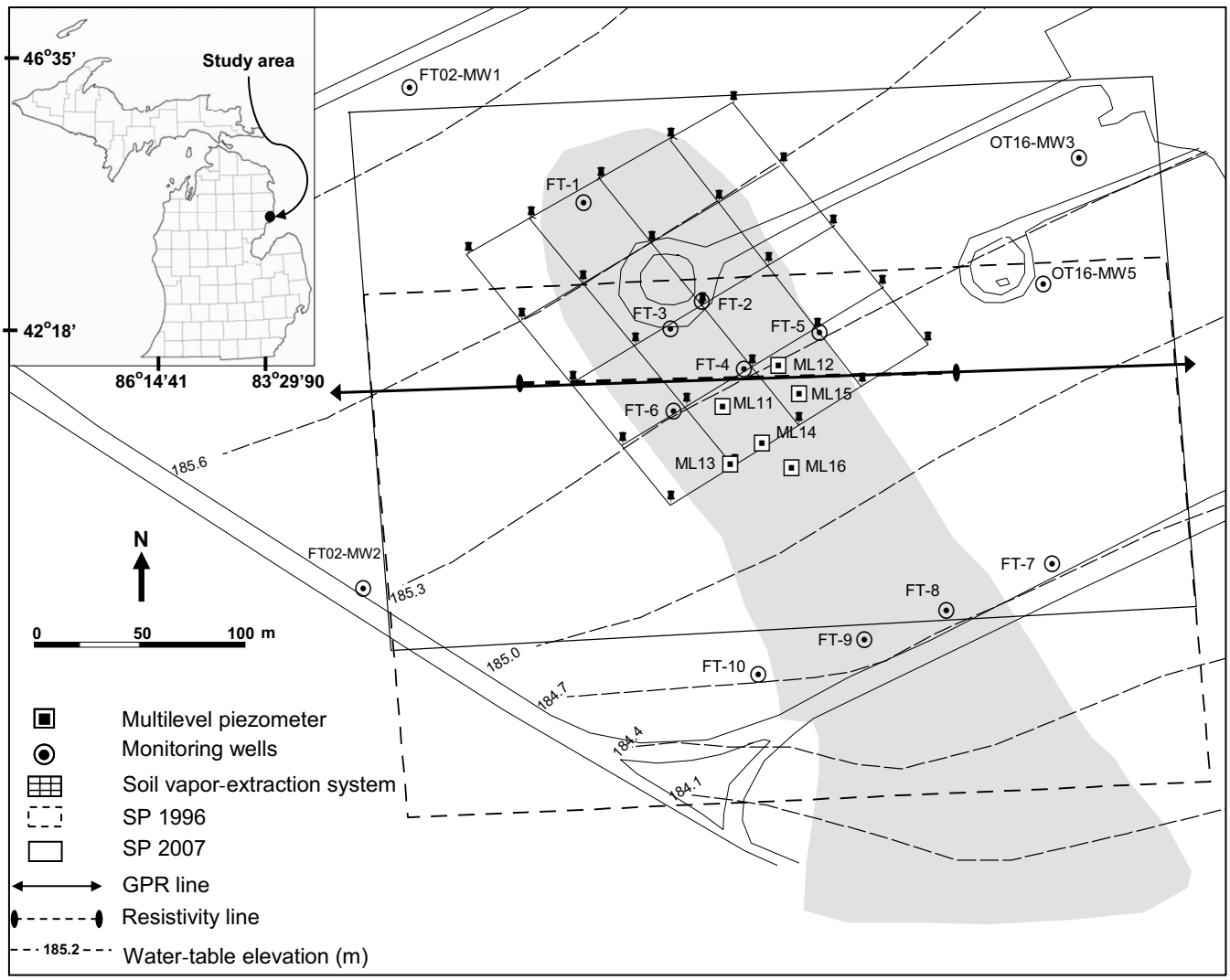

Figure 2. Map of the FT-02 site, showing locations of electrical resistivity and GPR lines, SP grids, multilevel piezometers, monitoring wells, and SVE system. Gray area represents the outline of the FT-02 contaminant plume defined in 1996. A map of Michigan is inset.

between the surveys was not produced. Survey data collected in 1996 and 2003 were retrieved and clipped to display parts of the survey common with the 2007 survey. Data from all of the surveys were plotted using the same color scale to allow for direct comparison.

SP measurements (see Figure 2 for grid location) were conducted in 1996 and 2007 using nonpolarizable Cu-$CuSO_4$ electrodes and a high-impedance voltmeter. The potential difference was measured between a fixed reference electrode and a roving electrode placed at grid nodes established every 15.24 m. Because of difficulties in locating the 1996 survey boundary, the 2007 grid was offset from the 1996 grid approximately 100 m to the north (Figure 2). SP data were gridded using kriging and contoured using Surfer® software. We used the same color scale to plot the 1996 and 2007 data.

The GPR survey line established in 1996 was reoccupied in 2003 and 2007 (see Figure 2 for profile location). We conducted the survey using a GSSI Sir 10 A+ system. We used a 100-MHz bistatic antennas and recorded for a total of 400 ns. The 100-MHz transmitter-receiver pair was set at a fixed separation of 1.4 m between centers. We kept acquisition parameters for all three surveys constant: 512 samples/scan, 20 scans/second (14.7 scans/m), three-stage vertical (along scan) infinite impulse response (IIR) low-pass filter at 120 cycles/400 ns (300 MHz), and four-stage vertical IIR high-pass filter at 15 cycles/400 (37.5 MHz). We set gains automatically at the starting point of the survey, which was the same location for all three surveys, to equalize amplitudes to approximately 80% of full scale. The gains remained fixed for the entire survey. We processed the data using RADAN™ software. Low-frequency ringing and high-frequency noise across the profiles were eliminated. We plotted data from all surveys using the same color scale (amplitude to color conversion).

Chemical analysis of groundwater

NCIBRD constructed several monitoring wells and multilevel piezometers at the FT-02 site for groundwater sampling (Figure 2). Groundwater from monitoring wells and multilevel piezometers was pumped to the surface using a peristaltic pump. The water was pumped through a flow cell into which a YSI multiparameter probe was immersed. Water temperature, specific conductance (SPC), pH, and oxidation reduction potential (ORP) were recorded after the readings stabilized. Water samples were filtered using a 0.45-μm pore-size inline filter before collecting water for chemical and isotopic analyses. Ferrous iron (Fe^{2+}) was analyzed immediately after filtering in the field by colorimetry using the phenanthroline method (CHEMetrics Inc., 2004).

Samples for major ions were collected in polyethylene bottles (preacidified for cations), cooled to 4 °C on ice, and transported to the laboratory. Sulfate and calcium were analyzed by ion chromatography. Water for the stable carbon isotope ratio ($\delta^{13}C$) was collected and analyzed using the technique described by Atekwana and Krishnamurthy (1998). In addition, historical data (depth to water table, total petroleum hydrocarbons, and specific conductance) used in this study were obtained from the Wurtsmith Air Force Base (WAFB) Authority.

RESULTS

Geophysical data

Electrical resistivity (ER) data acquired in 1996 and 2003 are reported in Sauck et al. (1998) and Smart et al. (2004), respectively. A compilation of the inverted resistivity profile acquired from 1996, 2003, and 2007 is presented in Figure 3. The 1996 resistivity results show a region of lower resistivity coincident with the zone of contamination (horizontal coordinates 70-40 m), extending from near the surface into the saturated zone (Figure 3a). Within this low-resistivity region, the apparent resistivities are <700 ohm-m and decrease with depth to ~100 ohm-m. Resistivity values in the uncontaminated regions of the vadose zone are greater than 2000 ohm-m. The 2003 resistivity survey result shows a zone of low resistivity over the plume region between 100 and 170 m (Figure 3b). However, the highest resistivity values within the contaminated region of roughly 700 ohm-m in the 1996 survey increased to approximately 1200 ohm-m in 2003 (Figure 3a versus b).

Results of the 2007 survey (Figure 3c) differ markedly from the 1996 and 2003 surveys (Figure 3a and b). The low-resistivity anomaly observed in the vadose zone over the plume region in 1996 and 2003 is not evident in 2007 data. Instead, the previously anomalous conductive zone has become more resistive and reverted to near-background resistivity values of about 2500 ohm-m (Figure 3c). The anomalous conductive zone within the saturated zone over the plume is barely visible on the 2007 resistivity profile. We observe a uniform (~1.5-m-thick) lower resistivity (1000–2000 ohm-m) at the surface, which we attribute to precipitation recharge. Up to 4.8 cm of rain had fallen two weeks prior to our survey (Weather Underground, 2008).

Sauck et al. (1998) report SP data acquired in 1996. The 1996 SP data show a northwest-southeast-trending positive anomaly (8–24 mV) approximately 80 m wide and more than 250 m long, which is coincident with the region of groundwater contamination (Figure 4a) and the zone of anomalous conductivity (Figure 3a). However, the 2007 survey area (Figure 4b) is characterized by more negative SP values between −18 and −34 mV over the plume area observed in 1996.

GPR data acquired in 1996 and 2003 are reported in Sauck et al. (1998) and Smart et al. (2004), respectively. The 1996 GPR profile shows strong reflectors at approximately 100 ns, coincident with the elevation of the water table (Figure 5a). Sauck et al. (1998) suggest that strong reflectors at the water table are from the large change in relative permittivity from moist sand (ε_r~9) to saturated sand (ε_r ~25).

As noted by Sauck et al. (1998) and Bradford (2007), the most prominent feature of the GPR record is a region of attenuated amplitudes (a shadow zone). This zone of attenuated reflections (60–75 m wide) begins just below the water table and extends the full length of the record. Sauck et al. (1998) use this attenuation anomaly to define the transverse extent of the plume over the entire site (see Figure 3 in Sauck et al., 1998). The attenuation anomaly observed in the 1996 GPR profile (Fig 5a) is also evident in the 2003 and 2007 records (Figure 5b and c), with some notable differences within the contaminated zone. In the 2007 profile, the zone of attenuation occurs deeper in the record (~150 ns) and appears to be wider when compared to 1996 and 2003 data. Also, GPR reflectors at the water table and immediately below the water table are stronger when compared to GPR reflectors in 1996 and 2003 (Figure 5c).

Geochemical data

Figure 6 shows geochemical parameters in groundwater collected from multilevel piezometers in 2007. We observe negative Eh (Fig-

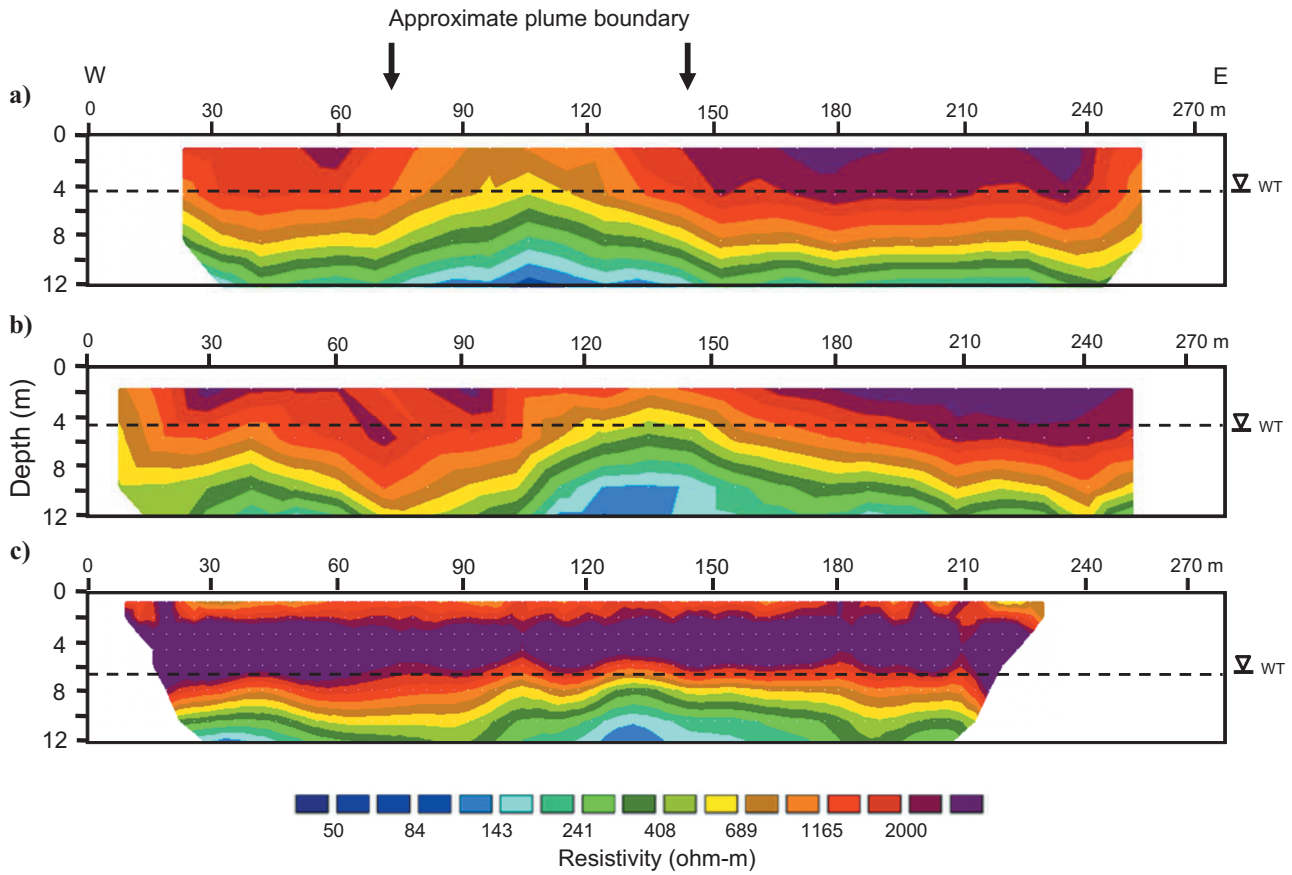

Figure 3. Inverted dipole-dipole resistivity profiles along the contaminant plume for (a) 1996, (b) 2003, and (c) 2007, respectively. Arrows indicate the approximate lateral extent of the contaminant plume. Note the change in conductivity in the contaminant plume over time.

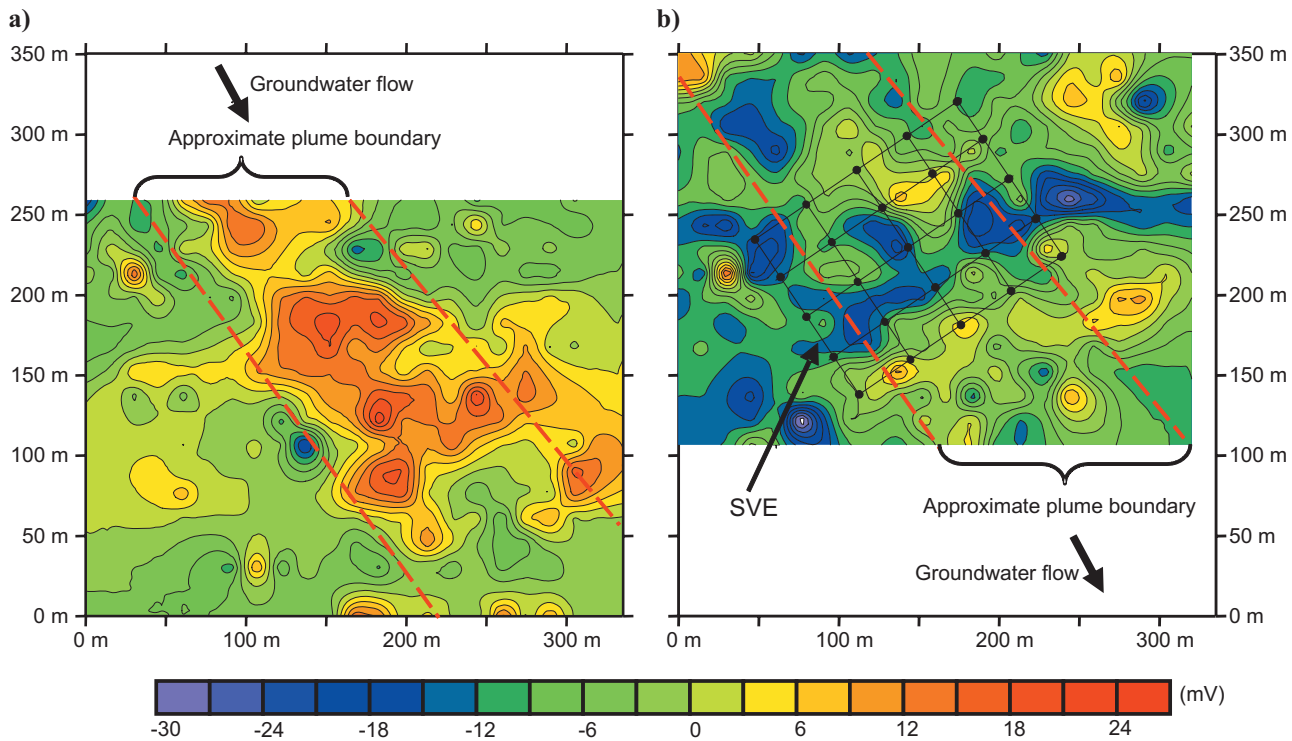

Figure 4. SP anomaly map of a portion of the FT-02 measured in (a) 1996 and (b) 2007. A grid showing the SVE system is superimposed on the 2007 SP grid.

ure 6a) and low dissolved-oxygen values within the contaminated aquifer, suggesting that anaerobic biodegradation is still occurring within the plume (Chapelle et al., 1996; Skubal et al., 1999; McGuire et al., 2000; Skubal et al., 2001; Moody et al., 2003). We also observe higher Fe^{2+} (~13 mg/l) and low sulfate concentrations (<2 mg/l) within the contaminated plume (Figure 6b and c). These redox zones defined by Eh, Fe^{2+}, and sulfate are coincident with positive $\delta^{13}C_{DIC}$, higher concentrations of calcium (>80 mg/l), and higher specific conductance (>400 μS/cm) (Figure 6d-f). The combined geochemical results suggest a 3-m contaminated zone below the water table in which biodegradation is active and where peaks in the different parameters occur about 1 m below the water table (Figure 6).

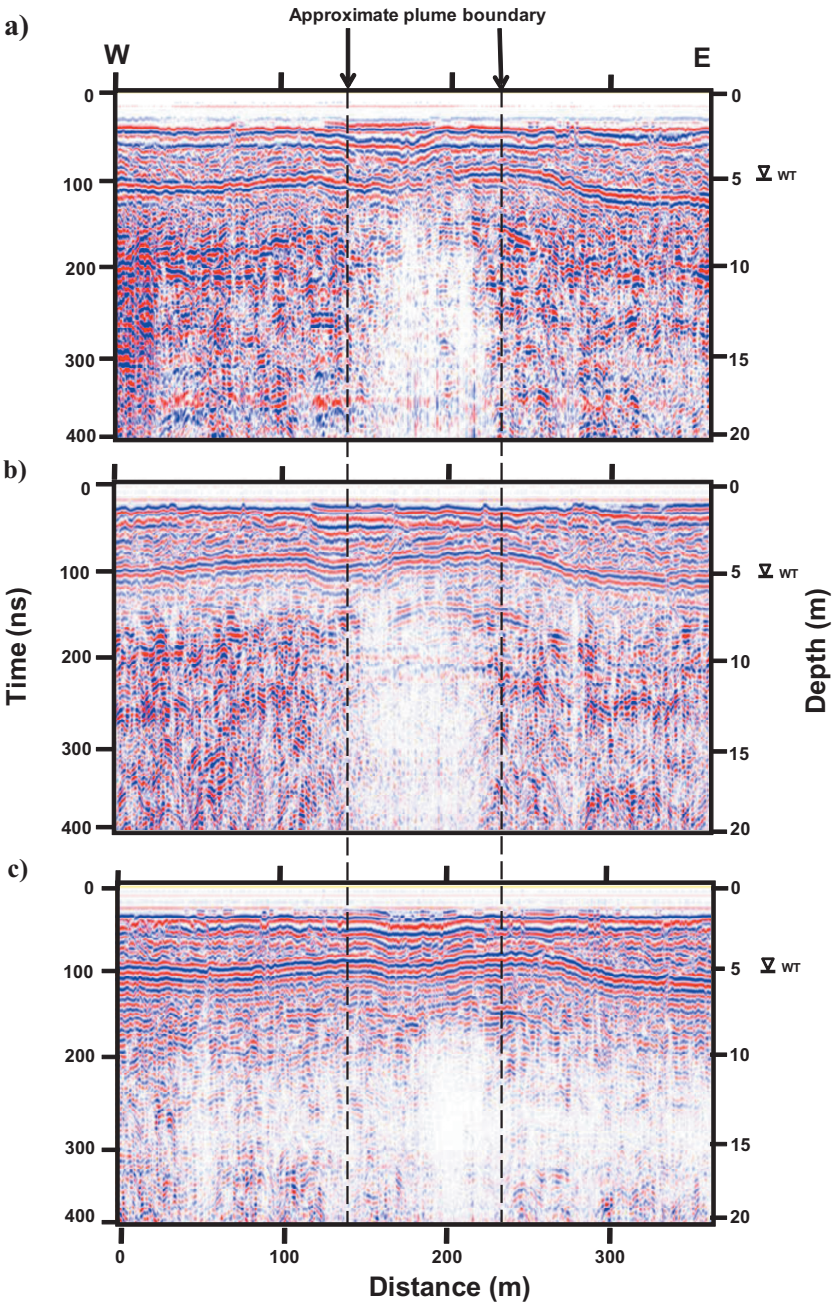

Figure 5. GPR profile over FT-02 contaminant plume measured in (a) 1996, (b) 2003, and (c) 2007. Arrows indicate the approximate lateral extent of the contaminant plume. Note the change in water-table reflectors around 100 ns and the change in depth of the shadow zone in the contaminant plume over time.

DISCUSSION

History of hydrocarbon contamination at the FT-02 site

Hydrocarbon contamination at the FT-02 site initially was investigated by ICF Kaiser Technology, Inc. (ICF) in 1995. Chemical analysis of groundwater showed volatile organic and semivolatile organic compounds (acenapthene, benzene, toluene, ethylbenzene, and xylenes) at concentrations ranging from 10 to 2000 mg/l (ICF, 1995). As much as 30 cm of the free product were observed above the water table during construction of monitoring wells more than 200 m downgradient of the contamination-source area (Figure 1). As part of the NCIBRD program, several studies have characterized the spatial extent of hydrocarbon contamination and the biological and chemical processes occurring in the contaminated media (e.g., Chapelle et al., 1996; Sauck et al., 1998; Skubal et al., 1999; McGuire et al., 2000; Skubal et al., 2001). These studies were instrumental in the remedial plan developed for the site.

In May 2001, the Wurtsmith Air Force Base Authority installed an SVE system over the FT-02 contaminant source area (Figure 2). The SVE system consists of 25 extraction points that remove volatile and semivolatile hydrocarbons by inducing vacuum conditions in the vadose zone. As of March 2003, approximately 2320 kg of free product had been extracted from the vadose zone (Parsons, 2004). Removal of hydrocarbon contaminants from the vadose zone of the source area by SVE is reflected in temporal groundwater chemistry.

We use historical data from monitoring well FT-4S in the source area and along our GPR and resistivity survey lines and monitoring well FT-8S located downgradient (Figure 2) to illustrate temporal changes in the contaminant plume. Prior to installation of the SVE system, total petroleum hydrocarbon (TPH) concentration in groundwater was as high as 650 μg/l in 2000 (Figure 7a). After installation, the TPH concentration in groundwater in the source area at FT-4S decreased steeply to approximately 100 μg/l in late 2002. Following this decrease, TPH concentrations fluctuated between 100 and 200 μg/l from 2002 to 2007. The TPH concentration in the groundwater at FT-8S generally mirrors that in the source area (Figure 7a).

During SVE system operation, the vacuum created by the system to cause volatilization of the hydrocarbon induces airflow into the vadose zone and aquifer. The supply of air provides oxy-

gen, which enhances aerobic biodegradation. Enhancement of biodegradation by oxygen brought to the contaminated zone by this process is observed in the sharp rise in groundwater temperature at FT-4S by about 5 °C between 2000 and late 2003 (Figure 7b). The water-temperature downgradient at FT-8S dropped initially between 2001 and 2003, shortly after the installation of the SVE system — perhaps because of a decrease in transport of the contaminant mass to downgradient locations (Figure 7b).

Decrease in the specific conductance within the contaminated aquifer measured at FT-4S and FT-8S generally mirrors the decrease in TPH (Figure 7c). Within the source area, specific conductance decreased from about 1000 μS/cm in 2001 to less than 300 μS/cm in 2003. However, the specific conductance between 2003 and 2007 fluctuated between 400 and 600 μS/cm, which we attribute to seasonal variations in rainfall recharge (Figure 7d). During periods of lower water table, the specific conductance is higher, and vice versa.

Hydrocarbon biodegradation and geophysical response

The physical contaminated environment is altered by growth and proliferation of microbes; microbial attachment to solid surfaces; production of biosurfactants, organic and carbonic acids, and various gases (e.g., CO_2, N_2); and mineral weathering and precipitation reactions. The expected geophysical response can vary and depends on the sensitivity of a specific geophysical technique to changes imposed on the physical property of the contaminant environment.

The geophysical surveys were conducted near the source area where the vadose zone and saturated zone were impacted by hydrocarbons (Figure 2). Investigations conducted in 1996 showed a distinct geoelectrically conductive anomaly within the saturated and unsaturated zones over the contaminant plume and coincident with the area of positive SP anomalies and attenuated GPR reflections (Figures 3a, 4a, and 5a). Geochemical data from contaminated groundwater at this site document microbial activity from terminal-electron-acceptor depletion, elevated pore-fluid conductivity, high calcium concentrations (Figure 6), and temporal increase in temperature (Figure 7b).

Although we did not investigate evidence of microbial activity within the capillary fringe and vadose zone with free product and residual product in this study, other studies have shown evidence of biodegradation and microbial activity effects on geophysical properties. In a laboratory column experiment where sediments were contaminated with diesel, Atekwana et al. (2004c) show higher bulk electrical conductivity in the region above the water table where sediments had free product and residual product saturation compared to the contaminated saturated zone with dissolved product. The population of microbes capable of degrading hydrocarbon was higher in the zone of highest bulk electrical conductivity above the water table (Atekwana et al., 2004c). Similar observations of higher bulk electrical conductivity and hydrocarbon degrading microbial population have been reported in field settings (Werkema et al., 2003; Atekwana et al., 2004d; Allen et al., 2007). Werkema et al. (2003) estimate pore-water conductivity ratios between contaminated and uncontaminated locations of 5.5 in the smear zone (contaminated region with free and residual product saturation that straddles the water table and affected by seasonal water-level fluctuations) and between one and two for the saturated zone contaminated with dissolved product.

The geophysical picture that emerges from these studies is one in which hydrocarbon degradation in the smear zone is distinct from that of the saturated zone in terms of the magnitude of the geophysical response. At the FT-02 site, we attribute the decrease in the bulk electrical conductivity, negative SP anomaly, and increased GPR signal strength observed in the 2007 survey compared to earlier surveys in 1996 and 2003 (see Figures 3–5) to the removal of hydrocarbons from the vadose zone by the SVE system. We argue that removal of volatile and semivolatile hydrocarbon in the contaminated vadose zone caused a decrease in organic carbon (electron donor to the microorganisms), which decreased microbial activity. The decrease in the microbial activity and its direct and indirect effects in the contaminated environment impacted the physical properties of the contaminated environment and the resulting geophysical signatures (e.g., Figure 1).

Bulk electrical conductivity

In the absence of hydrocarbon contamination, bulk electrical conductivity of the subsurface can vary because of saturation, depth to groundwater table, temperature, and concentrations of ions (salini-

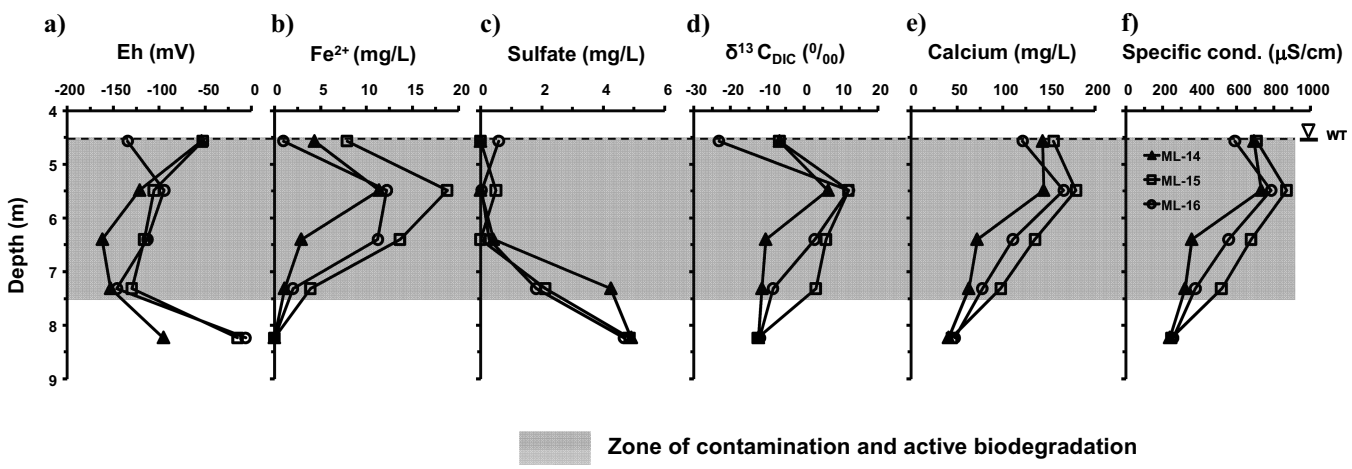

Figure 6. Depth variations of select chemical parameters: (a) oxidation reduction potential, (b) dissolved iron (Fe^{2+}), (c) sulfate, (d) carbon isotope of dissolved inorganic carbon ($\delta^{13}C_{DIC}$), (e) calcium, and (f) specific conductance measured in the contaminated aquifer in 2007 at the FT-02 site. The water table is at 4.5 m. The zone of active biodegradation was estimated from multilevel wells to be about 3 m.

ty) of pore fluids (e.g., Doser et al., 2004; Rein et al., 2004). For example, Rein et al. (2004) document short- to long-term variations in resistivity variations in an area of fluctuating groundwater level in response to rainfall events and seasonal and daily changes in temperature. The geophysical structure imaged shows up to 26% change in the resistivity in the uppermost soil layer (<1 m), which is ascribed to varying moisture changes and strong air-temperature variations (Rein et al., 2004). In dry climate settings where salts accumulate in the near surface because of evaporation, flushing of the salts by subsequent rains or irrigation is clearly evident in temporal resistivity imaging (e.g., Doser et al., 2004).

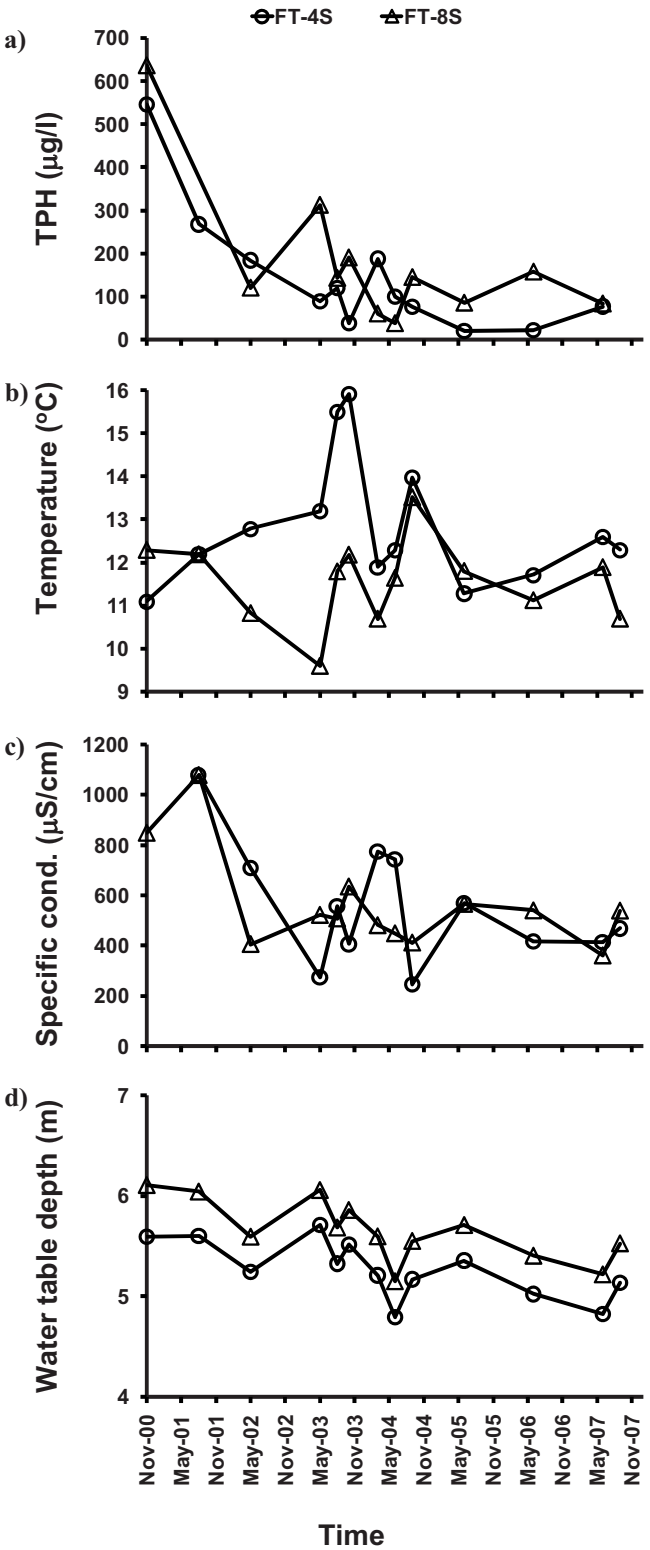

Figure 7. Temporal changes in (a) total petroleum hydrocarbon (TPH), (b) temperature, (c) groundwater specific conductance, and (d) depth to water table in the FT-02 contaminant plume.

Changes in the resistivity data presented in this study cannot be explained by both long-term and short-term variations in soil moisture, temperature, or pore-water salinity. Over the long term, groundwater levels have varied seasonally and annually (Figure 7d) but have remained within less than 1.0 m. Water temperature increased between 2000 and 2003 and has changed by only about 1 °C from 2003 to 2007 (Figure 7b). Additionally, the groundwater ionic chemistry indicated by the specific conductance has varied little between 2003 and 2007 except for seasonal water-level changes (Figure 7c). Two weeks before the 7 May 1996, 24 June 2003, and 1 September 2007 surveys were conducted, rainfall events totaling 3.6, 1.3, and 4.8 cm, respectively were recorded at the Alpena weather station (KAPN) 81-km north of the study site (Weather Underground, 2008).

The difference in rainfall totals in the two weeks prior to our surveys indicates a much wetter 2007, which should result in a lower-resistivity vadose zone. This is in contrast to our actual observation (Figure 3c). However, precipitation occurring prior to the 2007 survey can be seen in the resistivity section that shows a thin (<1 m), shallow, lower-resistivity layer extending across the entire section. Mean daily temperature for the two weeks prior to each survey were 3.6 °C in 1996, 16.6 °C in 2003, and 18.0 °C in 2007 (Weather Underground, 2008). The difference in the mean air temperature (<1.5 °C) is not sufficient to result in the more than 1000 ohm-m increase in resistivity between 2003 and 2007. The climate in the study area is humid, and there are no reported occurrences of salt formation in the surface soils that can impact the resistivity structure with rain recharge. Finally, the resistivity structures of the background areas are all above 2000 ohm-m; hence, we argue that temporal changes in the anomalous low-to-high resistivity over the contaminated zone cannot be explained by long- or short-term variations in moisture content, temperature, or salinity. Therefore, we conclude that changes in bulk electrical conductivity observed within the contaminated zone might be related to the removal of hydrocarbons in the vadose zone and decreased microbial activity.

Although the SVE system decreased the mass of the hydrocarbons in the vadose zone, hydrocarbons in the dissolved phase still persist in the saturated zone. Geochemical data suggest that anaerobic biodegradation occurs within a narrow zone less than 3 m thick in the aquifer (Figure 6), evidenced by the terminal-electron-acceptor concentrations (e.g., Fe^{2+}, SO_4^{2-}). This zone of biodegradation is accompanied by low pH, high CO_2, high silica and calcium concentrations, and high specific conductance. The higher silica and calcium concentration is evidence of enhanced mineral weathering within this zone in the aquifer (e.g., Atekwana et al., 2004d, Atekwana et al., 2005).

The 3-m-thick contaminated zone below the water table with higher specific conductance is not clearly evident on the 2007 resistivity profile (Figure 3c). To explain this observation, we performed a simple three-layer forward model (Figure 8) with a 3-m-thick bulk conductive layer in the upper parts of the saturated zone. Resistivity values assigned to the different layers were obtained from measure-

ments made on cores retrieved from the FT-02 site in 2007. Model-simulation results suggest that given a saturated plume thickness of approximately 3 m with an apparent resistivity of 273 ohm-m, a background saturated-zone apparent resistivity of 540 ohm-m, and a vadose-zone apparent resistivity of 1120 ohm-m, a bulk electrical conductivity anomaly is not evident in the modeled data (Figure 8a). This simulation result is similar to what we observe in the 2007 resistivity profile (Figure 3c).

However, when apparent resistivity of the contaminant plume in the saturated zone is decreased by approximately three to five times the background values, as suggested by Werkema et al. (2003), the bulk electrical conductivity anomaly is observed on the resistivity section (Figure 8b). Figure 8c shows the result of a forward model where we use apparent resistivity for the contaminant plume at 273 ohm-m, background-saturated-zone apparent resistivity of 540 ohm-m, and a vadose-zone apparent resistivity of 1120 ohm-m. However, we extend the 3-m contaminant plume in the saturated zone into the vadose zone by 2 m. Simulation results show a visible conductive plume in the modeled resistivity sections. Forward-model results suggest that bulk electrical conductivity of the 3 -m-thick layer in the saturated zone must be at least four to five times higher than background bulk conductivities or be extended into the vadose zone by about 2 m to be observed in the resistivity sections. Therefore, we conclude that the high-bulk electrical-conductivity anomaly observed in 1996 and 2003 occurred mainly because of vadose-zone contamination and accompanying biodegradation effects.

Self-potential

Terminal-electron-acceptor processes during microbial degradation of hydrocarbon are driven by redox conditions in the contaminated media (e.g., Vroblesky and Chapelle, 1994; Cozzarelli et al., 2001). The redox state within a hydrocarbon contamination differs significantly from background conditions. Naudet et al. (2003) and Naudet et al. (2004) suggest that SP anomalies in organic-rich contaminant plumes are generated in response to redox processes because of good positive correlations between Eh and residual SP. The relationship between SP versus Eh for the FT-02 site is poor ($R^2 = 0.0335$).

Our resistivity analysis suggests that the contaminated saturated and vadose zones contribute differently to the geophysical response measured at the surface and that the vadose-zone contribution to the geophysical response might be higher than that of the saturated zone. In fact, Minsley et al. (2007) show very strong SP (mean of 60 mV) signals for dense nonaqueous-phase liquids (DNAPL) trapped in the vadose zone, which they attribute to biodegradation. High SP values show close correspondence to high DNAPL concentration, although this was not entirely true for all locations at the study site (Minsley et al., 2007). Thus, the poor correlation we observe between SP and Eh at the FT-02 site could occur for two reasons: (1) redox measurements being compared to SP were collected from groundwater and might contribute only partly to the total SP measured at the surface; and (2) redox conditions occurring from biodegradation in the capillary fringe and lower vadose zone that might contribute to the overall electrochemistry of the system redox were not measured.

An alternative mechanism that might cause the observed SP is diffusion potentials arising from differences in the mobility of electrolytes of different concentrations in the contaminated and background pore fluids and groundwater (Telford et al., 1990; Reynolds, 1997; Nyquist and Corry, 2002). Such diffusion potentials typically are small and positive, consistent with the values observed in this study. Sauck et al. (1998) attributes the high SP source at the FT-02 plume to electrochemical potentials from chemical concentration gradients and ion diffusion. If SP is generated by ionic diffusion potential, then the steep decrease in SP between 1996 and 2007 cannot

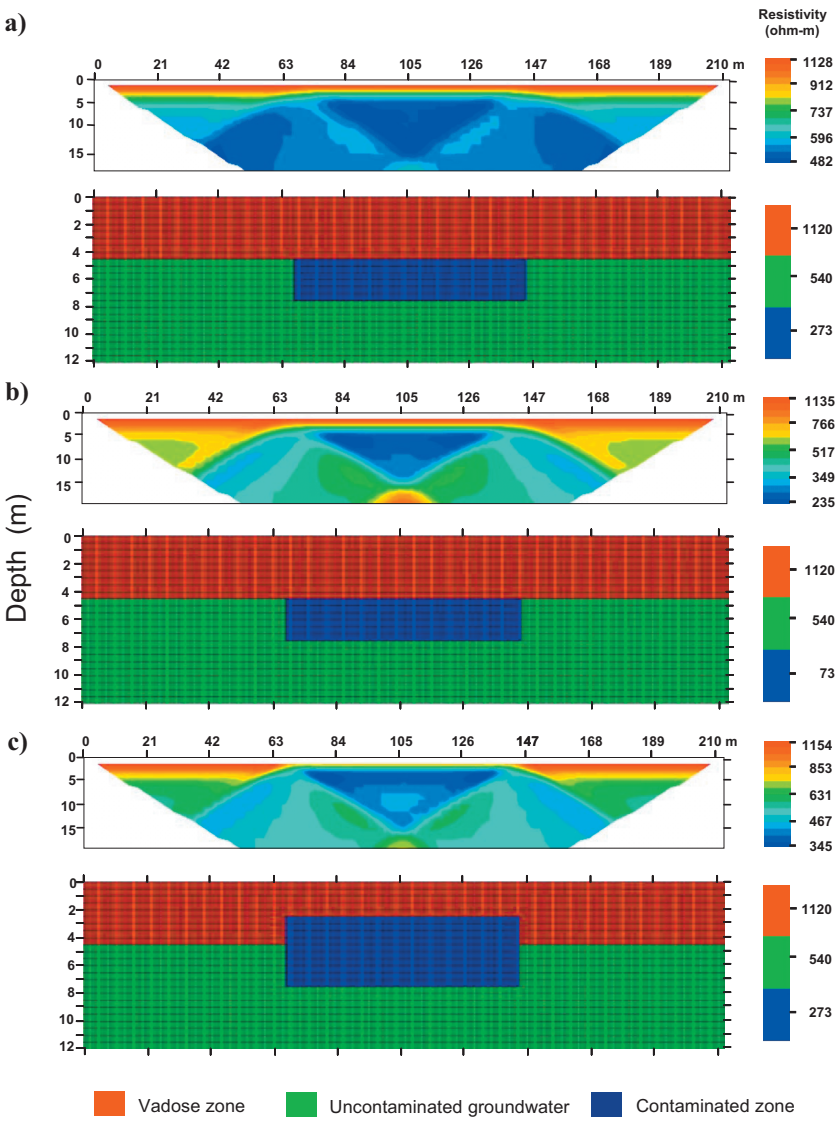

Figure 8. Forward model simulating different conductivity scenarios: (a) 3-m conductive plume with 273 ohm-m, (b) 3-m conductive plume with 73 ohm-m, and (c) 5-m conductive plume extending to the vadose zone.

be explained by ionic flushing by fresh water, an explanation used to account for lower bulk electrical conductivity along the profile in 2003 (Smart et al., 2004).

For the diffusion potentials to persist in natural settings, there must be a source/mechanism capable of maintaining imbalances in the electrolyte concentration (in our case, excess organic carbon that drives the hydrocarbon biodegradation) (Reynolds, 1997). Hence, any reduction in the ionic concentration over time also will reduce the magnitude of this potential. Removal of hydrocarbon mass by the SVE system decreases biodegradation activities. The decrease in microbial activities in turn decreases the ionic concentration differences between fluids in the contaminated and uncontaminated zones (vadose and saturated), explaining the observed decrease in SP between 1996 and 2007. Although streaming potentials arising from fluid flow (Telford et al., 1990) can cause an SP response, we discount this possibility at the site because of low groundwater gradients and velocity.

Ground-penetrating radar

Two main changes appear in the GPR records over the FT-02 contaminant plume from 1996 to 2007: (1) relative strengthening of GPR reflections (water-table reflection and reflections below the water table) with time and (2) lowering the depth of the shadow zone below the water table (Figure 5). In the absence of changing geologic parameters, variations of GRP attenuation over LNAPL plumes occur because of changing dielectric constants (relative permittivity contrast) and the resistivity structure of the subsurface (e.g., Daniels et al., 1995; Cassidy, 2007).

Attenuation of GPR reflection amplitude resulting in the shadow zone is explained by an increase in the bulk conductivity associated with biodegradation (e.g., Sauck, 2000; Bradford, 2007). Bradford (2007) suggests that increased conductivity in the contaminated-zone pore fluids alters the relaxation characteristics of the bulk formation, masking decrease in dispersion caused by the residual hydrocarbons. In addition, Bradford (2007) notes that dispersion in the zone of contamination is generally higher in the vadose zone than in the saturated zone (see Figure 8c in Bradford, 2007). Cassidy (2007) shows enhanced relative GPR signal attenuation associated with the smear zone surrounding the seasonally changing water-table interface compared to the saturated contaminated zone.

The zone of higher dispersion (Bradford, 2007) and enhanced signal attenuation (Cassidy, 2007) in the contaminated vadose zone corresponds to the same region of the vadose zone where we show elevated bulk electrical conductivity in our 1996 and 2003 resistivity surveys (Figure 3a and b). We infer that the predominant effect to the GPR signal attenuation occurs from microbial alteration of the contaminants. Thus, removal of hydrocarbon from the contaminant zone and reduction in fluid conductivity (Figure 7) could explain stronger GPR reflections. However, we are unable to explain why GPR attenuation is deeper and wider below the water table in the 2007 image than in the 2003 and 1996 images (Figure 3). Further investigation is needed to explain this phenomenon.

CONCLUSIONS

Removing the contaminant mass from the LNAPL-contaminated area altered the physiochemical and biological properties of the subsurface, which can be monitored using chemical analysis of groundwater and integrated geophysical techniques (GPR, SP, and electrical resistivity). Laboratory and field surveys have demonstrated increased bulk conductivities and increased microbial activities associated with LNAPL contamination. Geophysical signatures associated with long-term changes in contaminant reduction (e.g., by natural or engineered biodegradation or source removal) is unknown. In this study, we demonstrate that removing the contaminant mass from the source area reduced the TPH available for microbial metabolism, thereby altering the chemical, biological, and physical conditions in the aquifer. By removing the hydrocarbon source from the area, the microbial population and activity also reduce, resulting in changes that can be detected by geophysical techniques.

We suggest that contaminant mass reduction by natural bioremediation or engineered remediation can be imaged effectively using geophysical techniques, especially if contamination is prominent in the vadose zone. Nonetheless, in some field settings, microbial degradation and alteration of the contaminant mass and aquifer matrix might not be detected by geophysical techniques. Therefore, the applicability of our results to other sites must be governed by an understanding of (1) relative distribution and volume of different phases of LNAPL contamination, (2) the effect of changes in physical properties of contaminated media imparted by physical, chemical, and biological alteration of the contaminant, and (3) the ratio of the mass or volume of biologically altered aquifer matrix relative to the background.

ACKNOWLEDGMENTS

Partial funding for this work was provided by the National Science Foundation (grants EAR-0651433, OCE 0433869, and OCE 0729642) and the U. S. Environmental Protection Agency (EPA), grant RFQ-RT-07-00183A. The EPA, through its Office of Research and Development, funded and collaborated in the research described here under RFQ-RT-07-00183A to V. Che-Alota. It has been subjected to agency review and approved for publication. We thank Wurtsmith Air Force Base authorities and Paul Rekowski for allowing us access to the site. Charles Major provided the historical groundwater chemistry data. We thank Caroline Davis, Jay Nolan, Ryan Joyce, Silvia Rossbach, and Gamal Abdel Aal for their help with data collection and processing. We also thank four anonymous reviewers whose comments helped to improve this manuscript.

REFERENCES

Abdel Aal, G. Z., E. A. Atekwana, S. Radzikowski, and S. Rossbach, 2009, Effect of bacterial adsorption on low frequency electrical properties of clean quartz sands and iron-oxide coated sands: Geophysical Research Letters, **36**, L04403.

Abdel Aal, G. Z., E. A. Atekwana, L. D. Slater, and E. A. Atekwana, 2004, Effects of microbial processes on electrolytic and interfacial electrical properties of unconsolidated sediments: Geophysical Research Letters, **31**, L12505.

Abdel Aal, G. Z. , L. D. Slater, and E. A. Atekwana, 2006, Induced-polarization measurements on unconsolidated sediments from a site of active hydrocarbon biodegradation: Geophysics, **71**, no. 2, H13–H24.

Allen, P. J., E. A. Atekwana, E. A. Atekwana, W. J. Duris, D. D. Werkema, and S. Rossbach, 2007, The microbial community structure in petroleum-contaminated sediments corresponds to geophysical signatures: Applied and Environmental Microbiology, **73**, 2860–2870.

Atekwana, E. A., E. A. Atekwana, F. D. Legall, and R. V. Krishnamurthy, 2004a, Field evidence for geophysical detection of subsurface zones of enhanced microbial activity: Geophysical Research Letters, **31**, L23603.

——–, 2005, Biodegradation and mineral weathering controls on bulk electrical conductivity in a shallow hydrocarbon contaminated aquifer: Journal of Contaminant Hydrology, **80**, 149–167.

Atekwana, E. A., E. A. Atekwana, R. S. Rowe, D. D. Werkema, and F. D. Legall, 2004b, Total dissolved solids in groundwater and its relationship to bulk electrical conductivity of soils contaminated with hydrocarbon: Jour-

nal of Applied Geophysics, **56**, 281–294.
Atekwana, E. A., E. A. Atekwana, D. D. Werkema, J. P. Allen, L. A. Smart, J. W. Duris, D. P. Cassidy, W. A. Sauck, and S. Rossbach, 2004c, Evidence for microbial enhanced electrical conductivity in hydrocarbon-contaminated sediments: Geophysical Research Letters, **31**, L23501.
Atekwana, E. A., and R. V. Krishnamurthy, 1998, Seasonal variations of dissolved inorganic carbon and $\delta^{13}C$ of surface waters: Application of a modified gas evolution technique: Journal of Hydrology, **205**, 265–278.
Atekwana, E. A., W. A. Sauck, and D. D. Werkema, 2000, Investigations of geoelectrical signatures at a hydrocarbon contaminated site: Journal of Applied Geophysics, **44**, 167–180.
Atekwana, E. A., D. D. Werkema, J. W. Duris, S. Rossbach, E. A. Atekwana, W. A. Sauck, D. P. Cassidy, J. Means, and F. D. Legall, 2004d, In-situ apparent conductivity measurements and microbial population distribution at a hydrocarbon contaminated site: Geophysics, **69**, 56–63.
Baedecker, M. J., I. M. Cozzarelli, R. P. Eganhouse, D. I. Siegel, and P. C. Bennett, 1993, Crude oil in a shallow sand and gravel aquifer — III: Biogeochemical reactions and mass balance modeling in anoxic groundwater: Applied Geochemistry, **8**, 569–586.
Bennett, P. C., F. K. Hiebert, and W. J. Choi, 1996, Microbial colonization and weathering of silicates in a petroleum-contaminated groundwater: Chemical Geology, **132**, 45–53.
Benson, A. K., K. L. Payne, and M. A. Stubben, 1997, Mapping groundwater contamination using dc resistivity and, VLF geophysical methods — A case study: Geophysics, **62**, 80–86.
Bermejo, J. L., W. A. Sauck, and E. A. Atekwana, 1997, Geophysical discovery of a new LNAPL plume at the former Wurtsmith, AFB, Oscoda, Michigan: Ground Water Monitoring and Remediation, **17**, 131–137.
Bradford, J. H., 2007, Frequency-dependent attenuation analysis of ground-penetrating radar data: Geophysics, **72**, no. 4, J7–J16.
Cassidy, N. J., 2007, Evaluating LNAPL contamination using, GPR signal attenuation analysis and dielectric property measurements: Practical implications for hydrological studies: Journal of Contaminant Hydrology, **94**, 49–75.
——–, 2008, GPR attenuation and scattering in a mature hydrocarbon spill: A modeling study: Vadose Zone Journal, **7**, 140–159.
Chapelle, F. H., S. K. Haack, P. Adriaens, M. A. Henry, and P. M. Bradley, 1996, Comparison of E(h) and H-2 measurements for delineating redox processes in a contaminated aquifer: Environmental Science and Technology, **30**, 3565–3569.
CHEMetrics Inc., 2004, V-2000 photometer operator's manual.
Cozzarelli, I. M., B. A. Bekins, M. J. Baedecker, G. R. Aiken, R. P. Eganhouse, and M. E. Tuccillo, 2001, Progression of natural attenuation processes at a crude oil spill site: 1. Geochemical evolution of the plume: Journal of Contaminant Hydrology, **53**, 369–385.
Cozzarelli, I. M., R. P. Eganhouse, and M. J. Baedecker, 1990, Transformation of monoaromatic hydrocarbons to organic acids in anoxic groundwater environment: Environmental Geology and Water Science, **16**, 135–141.
Daniels, J. J., R. Roberts, and M. Vendl, 1995, Ground-penetrating radar for the detection of liquid contaminants: Journal of Applied Geophysics, **33**, 195–207.
Davis, C. A., E. A. Atekwana, E. A. Atekwana, L. D. Slater, S. Rossbach, and M. R. Mormile, 2006, Microbial growth and biofilm formation in geologic media is detected with complex conductivity measurements: Geophysical Research Letters, **33**, L18403.
de la Vega, M., A. Osella, and E. Lascano, 2003, Joint inversion of Wenner and dipole-dipole data to study a gasoline-contaminated soil: Journal of Applied Geophysics, **54**, 97–109.
Doser, I. D., O. S. Dena-Ornelas, R. P. Langford, and M. R. Baker, 2004, Monitoring yearly changes and their influence on electrical properties of the shallow subsurface at two sites near the Rio Grande, West Texas: Journal of Environmental and Engineering Geophysics, **9**, 179–190.
Endres, A. L., and J. D. Redman, 1996, Modeling the electrical properties of porous rocks and soils containing immiscible contaminants: Journal of Environmental and Engineering Geophysics, **0**, 105–112.
Halihan, T., S. Paxton, I. Graham, T. Fenstemaker, and M. Riley, 2005, Post-remediation evaluation of a LNAPL site using electrical resistivity imaging: Journal of Environmental Monitoring, **7**, 283–287.
ICF Technology Inc., 1995, The United States Air Force installation restoration program: Draft remedial investigation report, sites FT-02, OT-16, and LF-27: Wurtsmith Air Force Base, **1**, ICF Technology, Inc.
Kaufmann, O., and J. Deceuster, 2007, A 3D resistivity tomography study of a LNAPL plume near a gas station at Brugelette (Belgium): Journal of Environmental and Engineering Geophysics, **12**, 207–219.
Loke, M. H., and R. D. Baker, 1996, Rapid least-squares inversion of apparent resistivity pseudosections by a quasi-Newton method: Geophysical Prospecting, **44**, 131–152.
McGuire, J. T., E. W. Smith, D. T. Long, D. W. Hyndman, S. K. Haack, M. J. Klug, and M. A. Velbel, 2000, Temporal variations in parameters reflecting terminal-electron-accepting processes in an aquifer contaminated with waste fuel and chlorinated solvents: Chemical Geology, **169**, 471–485.
McMahon, P. B., D. A. Vroblesky, P. M. Bradley, F. H. Chapelle, and C. D. Gullett, 1995, Evidence for enhanced mineral dissolution in organic acid-rich shallow ground water: Ground Water, **31**, 207–216.
Minsley, B. J., J. Sogade, and F. D. Morgan, 2007, Three-dimensional self-potential inversion for subsurface DNAPL contaminant detection at the Savannah River site, South Carolina: Water Resources Research, **43**, W04429.
Moody, C. A., G. N. Hebert, S. H. Strauss, and J. A. Field, 2003, Occurrence and persistence of perfluorooctanesulfonate and other perfluorinated surfactants in groundwater at a fire-training area at Wurtsmith Air Force Base, Michigan, USA: Journal of Environmental Monitoring, **5**, 341–34.
Naudet, V., A. Revil, J.-Y. Bottero, and P. Begassat, 2004, Relationship between self-potential (SP) signals and redox conditions in contaminated groundwater: Geophysical Research Letters, **30**, 2091.
Naudet, V., A. Revil, E. Rizzo, J.-Y. Bottero, and P. Begassat, 2003, Groundwater redox conditions and conductivity in a contaminant plume from geoelectric investigations: Hydrology and Earth System Sciences, **8**, 8–22.
Nyquist, J. E., and C. E. Corry, 2002, Self-potential: The ugly duckling of the environmental geophysics: The Leading Edge, **21**, 446–451.
Parsons, 2004, First five-year review report for installation restoration program sites at Wurtsmith Air Force Base, Township of Oscoda, Iosco County, Michigan: Air Force Real Property Agency and Air Force Center for Environmental Excellence.
Rein, A., R. Hoffmann, and P. Dietrich, 2004, Influence of natural time-dependent variations of electrical conductivity on DC resistivity measurements: Journal of Hydrology, **285**, 215–232.
Reynolds, J. M., 1997, An introduction to applied and environmental geophysics: Wiley Interscience.
Sauck, W., 2000, A. model for the resistivity structure of LNAPL plumes and their environs in sandy sediments: Journal of Applied Geophysics, **44**, 151–165.
Sauck, W. A., E. A. Atekwana, and M. S. Nash, 1998, High conductivities associated with an LNAPL plume imaged by integrated geophysical techniques: Journal of Environmental and Engineering Geophysics, **2**, 203–212.
Skubal, K. L., M. J. Barcelona, and P. Adriaens, 2001, An assessment of natural biotransformation of petroleum hydrocarbons and chlorinated solvents at an aquifer plume transect: Journal of Contaminant Hydrology, **49**, 151–169.
Skubal, K. L., S. K. Haack, L. J. Forney, and P. Adriaens, 1999, Effects of dynamic redox zonation on the potential for natural attenuation of trichloroethylene at a fire-training-impacted aquifer: Physics and Chemistry of the Earth B, **24**, 517–527.
Smart, L., M. S. Nash, and W. A. Sauck, 2004, Wurtsmith Air Force Base revisited, 2004 Symposium on the Application of Geophysics to Engineering and Environmental Problems (SAGEEP), Proceedings, 374–385.
Telford, W. M., L. P. Geldart, and R. E. Sheriff, 1990, Applied geophysics: Cambridge University Press.
U.S. Geological Survey, 1991, Wurtsmith Air Force Base, Michigan: Investigations of groundwater and soil contamination at selected sites.
Vroblesky, D. A., and F. H. Chapelle, 1994, Temporal and spatial changes of terminal electron acceptor processes in petroleum hydrocarbon-contaminated aquifer and the significance for contaminant biodegradation: Water Resources Research, **30**, 1561–1570.
Werkema, D. D., E. A. Atekwana, L. E. Anthony, W. A. Sauck, and D. P. Cassidy, 2003, Investigating the geoelectrical response of hydrocarbon contamination undergoing biodegradation: Geophysical Research Letters, **30**, 49-1–49-4.
Weather Underground, 2008, Weather history for Alpina MI, http://www.wunderground.com/history/airport/kapn, accessed 29 April 2009.
Yang, C. H., C. Y. Yu, and S. W. Su, 2007, High resistivities associated with a newly formed LNAPL plume imaged by geoelectric techniques — A case study: Journal of the Chinese Institute of Engineers, **30**, 53–6.